

Measure synchronization in a spin-orbit-coupled bosonic Josephson junction

Wen-Yuan Wang,^{1,2} Jie Liu,^{1,2,3} and Li-Bin Fu^{2,3,*}

¹School of Physics, Beijing Institute of Technology, Beijing 100081, China

²National Laboratory of Science and Technology on Computational Physics,

Institute of Applied Physics and Computational Mathematics, Beijing 100088, China

³Center for Applied Physics and Technology, Peking University, Beijing 100084, China

(Received 19 May 2015; published 10 November 2015)

We present measure synchronization (MS) in a bosonic Josephson junction with spin-orbit coupling. The two atomic hyperfine states are coupled by a Raman dressing scheme, and they are regarded as two orientations of a pseudo-spin-1/2 system. A feature specific to a spin-orbit-coupled (SOC) bosonic Josephson junction is that the transition from non-MS to MS dynamics can be modulated by Raman laser intensity, even in the absence of interspin atomic interaction. A phase diagram of non-MS and MS dynamics as functions of Raman laser intensity and Josephson tunneling amplitude is presented. Taking into account interspin atomic interactions, the system exhibits MS breaking dynamics resulting from the competition between intraspin and interspin atomic interactions. When interspin atomic interactions dominate in the competition, the system always exhibits MS dynamics. For interspin interaction weaker than intraspin interaction, a window for non-MS dynamics is present. Since SOC Bose-Einstein condensates provide a powerful platform for studies on physical problems in various fields, the study of MS dynamics is valuable in researching the collective coherent dynamical behavior in a spin-orbit-coupled bosonic Josephson junction.

DOI: [10.1103/PhysRevA.92.053608](https://doi.org/10.1103/PhysRevA.92.053608)

PACS number(s): 03.75.Mn, 05.45.Xt, 64.60.-i

I. INTRODUCTION

In the 17th century, Huygens first observed synchronization in two pendulum clocks [1]. This phenomenon of synchronization is encountered in many different systems in nature and science. Classically, synchronization is defined as the frequency and phase locking of periodic oscillators due to weak interaction [2]. Although synchronization was first mentioned in periodic systems, synchronization in chaotic systems has attracted more attention due to its rich dynamical properties and potential applications in practical systems [3–10]. Since synchronization between two trajectories is normally related to the contraction of phase-space volume, it was explored mostly in dissipative systems in most related work.

In coupled nondissipative Hamiltonian systems, a new kind of synchronization, called measure synchronization (MS), was found by Hampton and Zanette [11]. MS occurs when all orbits of two coupled Hamiltonian systems cover the same region in phase space with identical invariant measures [2,11]. The transition from non-MS to MS in coupled Hamiltonian systems is characterized by coupling strength. As most important problems in both classical and quantum mechanics can be approximated by a Hamiltonian system, MS in coupled Hamiltonian systems is very important to understand the behavior of such systems. MS in coupled Hamiltonian systems has aroused considerable interest among researchers in areas such as coupled φ^4 -, Duffing-, and Frenkel-Kontorova-type Hamiltonian systems [2,12–15], as well as a bosonic Josephson junction [16–18].

More recently, due to the experimental realization of spin-orbit coupling in spinor Bose gases [19–24] and Fermi gases [25–27], the dynamics of spin-orbit-coupled (SOC) bosonic Josephson junction has been investigated [28–32]. In

addition to interspin atom interaction, two atomic hyperfine states are coupled by Raman coupling strength in an SOC bosonic Josephson junction. The experimental achievements of SOC quantum gases have stimulated a growing interest in the ultracold physics community in such areas as quantum phase transition [33], topological excitations [34], Majorana fermions [35], the spin Hall effect [36–39], and spintronic devices [40]. An SOC bosonic Josephson junction provides insight into the phenomena of the interplay between interatomic interaction and spin-orbit coupling, and thus it serves as a platform for quantum simulation and is worth more in-depth investigation.

In this paper, we study MS dynamics in a tunable SOC bosonic Josephson junction. The two atomic hyperfine states are coupled by Raman coupling strength in the system, which are regarded as the two orientations of a pseudo-spin-1/2 system. Without considering interspin atomic interaction, the dynamics of two coupled Hamiltonian systems exhibits a transition from non-MS to MS as the Raman coupling strength increases. The critical Raman laser intensity for the transition from non-MS to MS dynamics is dependent on the Josephson tunneling amplitude. Considering the interspin atomic interaction, the system displays MS breaking dynamics resulting from the competition between intraspin and interspin atomic interactions. The system always exhibits MS dynamics when the interspin atomic interaction is stronger than the intraspin atomic interaction. For interspin atomic interaction weaker than intraspin atomic interaction, a window for MS breaking dynamics is presented. The phase diagrams for MS breaking dynamics are obtained, which are helpful for controlling the measure synchronization of two atomic hyperfine states in the SOC bosonic Josephson junction.

The outline of the paper is as follows. In Sec. II, we introduce the Hamiltonian of an SOC bosonic Josephson junction. Following this, the main results are shown in Sec. III, which contains a Raman laser intensity induced transition from

*lbfu@iapcm.ac.cn

non-MS to MS dynamics and MS breaking dynamics. Finally, we present a summary and conclusion in Sec. IV.

II. HAMILTONIAN AND DYNAMIC DESCRIPTION OF AN SOC BOSONIC JOSEPHSON JUNCTION

Recently, spin-orbit coupling in ultracold ^{87}Rb atoms was realized experimentally at NIST [19]. In that experiment, the Raman dressing scheme was based on coupling two atomic hyperfine states of $5S_{1/2}$, $|F = 1, m_F = 0\rangle$ and $|F = 1, m_F = -1\rangle$, labeled as spin-up $|\uparrow\rangle$ and spin-down $|\downarrow\rangle$, respectively. We consider such an SOC BEC in a double-well potential, with the wells indicated by l and r , respectively. To investigate the dynamics of the system, we adopt the two-mode approximation [41–56]. The field operator $\hat{\Psi}_\sigma(x) \simeq \hat{a}_{l\sigma} \psi_{l\sigma} + \hat{a}_{r\sigma} \psi_{r\sigma}$ can be written in terms of the annihilation operators $\hat{a}_{j\sigma}$ at the j well ($j = l, r$) with spin σ ($\sigma = \uparrow, \downarrow$), where $\psi_{j\sigma}$ is the ground-state wave function of the j well with spin σ . Then, the total Hamiltonian for such an SOC BEC in a symmetrical double-well potential can be written as [28–32,57–59]

$$\hat{H} = \hat{H}_\uparrow + \hat{H}_\downarrow + \hat{H}_{\uparrow\downarrow}, \quad (1)$$

where

$$\begin{aligned} \hat{H}_\uparrow &= -J_{\uparrow\uparrow}(\hat{a}_{l\uparrow}^\dagger \hat{a}_{r\uparrow} + \hat{a}_{l\uparrow} \hat{a}_{r\uparrow}^\dagger) + \frac{u_{\uparrow\uparrow}}{2} \sum_j (\hat{a}_{j\uparrow}^\dagger \hat{a}_{j\uparrow}^\dagger \hat{a}_{j\uparrow} \hat{a}_{j\uparrow}), \\ \hat{H}_\downarrow &= -J_{\downarrow\downarrow}(\hat{a}_{l\downarrow}^\dagger \hat{a}_{r\downarrow} + \hat{a}_{l\downarrow} \hat{a}_{r\downarrow}^\dagger) + \frac{u_{\downarrow\downarrow}}{2} \sum_j (\hat{a}_{j\downarrow}^\dagger \hat{a}_{j\downarrow}^\dagger \hat{a}_{j\downarrow} \hat{a}_{j\downarrow}), \\ \hat{H}_{\uparrow\downarrow} &= -\Omega(\hat{a}_{l\uparrow}^\dagger \hat{a}_{l\downarrow} + \hat{a}_{r\uparrow}^\dagger \hat{a}_{r\downarrow} + \text{H.c.}) + u_{\uparrow\downarrow} \sum_j (\hat{a}_{j\uparrow}^\dagger \hat{a}_{j\downarrow}^\dagger \hat{a}_{j\uparrow} \hat{a}_{j\downarrow}). \end{aligned}$$

Here Ω is the Raman coupling strength, $J_{\sigma\sigma}$ is the Josephson tunneling amplitude between left and right wells, $u_{\sigma\sigma}$ is the intraspin atomic interaction, and $u_{\uparrow\downarrow}$ is the interspin atomic interaction. The double-well problem in the two-mode approximation results in terms containing $\hat{a}_{r\sigma}^\dagger \hat{a}_{r\sigma} \hat{a}_{l\sigma}^\dagger \hat{a}_{l\sigma}$ [41]. The terms just shift the critical values for the transition from non-MS to MS. Therefore, the terms are neglected for simplicity since they cannot change the MS.

The equations of motion can be easily obtained from the Heisenberg equation $i \frac{d}{dt} \hat{a}_{j\sigma} = [\hat{a}_{j\sigma}, \hat{H}]$. In this system, the total number N of particles is conserved. Under the mean-field approximation, the operator $a_{j\sigma}$ can be replaced by its expectation value $\langle \hat{a}_{j\sigma} \rangle$. For simplicity, we denote this c number with $a_{j\sigma}$. We thus obtain the following equations of motion:

$$i \frac{d}{dt} a_{j\sigma} = -J_{\sigma\sigma} a_{j'\sigma} - \Omega a_{j\sigma'} + g_{\sigma\sigma} |a_{j\sigma}|^2 a_{j\sigma} + g_{\sigma\sigma'} |a_{j\sigma'}|^2 a_{j\sigma}. \quad (2)$$

Here $j \neq j'$ and $\sigma \neq \sigma'$, $g_{\sigma\sigma} = N_\sigma u_{\sigma\sigma}$ is the nonlinear parameter describing the intraspin atomic interactions, and $g_{\uparrow\downarrow} = \sqrt{N_\uparrow N_\downarrow} u_{\uparrow\downarrow}$ is the nonlinear parameter describing the interspin atomic interaction. In the present paper, we use harmonic-oscillator dimensionless units ($\hbar = m = \omega = 1$). All lengths are now expressed in oscillator unit $\sqrt{\hbar/m\omega}$ and time in ω^{-1} .

In the present paper, we discuss the weakly interacting case, which meets the requirement of a two-mode approxi-

mation [41,42]. In the weakly interacting case, the mean-field analysis still works well. Since the parameters in the equations of motion (2) are all experimentally tunable, for simplicity we set both intraspin atomic interactions to be the same, i.e., $g_{\uparrow\uparrow} = g_{\downarrow\downarrow} = g$, and we also choose an equal Josephson tunneling amplitude $J_{\uparrow\uparrow} = J_{\downarrow\downarrow} = J$.

III. TRANSITIONS TO MS AND MS BREAKING DYNAMICS

If we do not consider Raman laser intensity, our mode is simplified to a two-species bosonic Josephson junction. MS dynamics in a two-species bosonic Josephson junction without spin-orbit coupling has been studied based on semiclassical theory [17] and quantum many-body systems [18]. It is found that the transition from non-MS to MS dynamics is mainly caused by the effective atomic interaction between different species. Because Raman laser intensity plays a crucial role in a spin-orbit-coupled bosonic Josephson junction, we first study its effect on the transition from non-MS to MS dynamics. Then, the effects of both terms, which couple the spin-up $|\uparrow\rangle$ and spin-down $|\downarrow\rangle$ system, on MS dynamics are investigated.

A. Raman laser intensity induced transition from non-MS to MS dynamics

MS and non-MS dynamics can be characterized by the domain covered during the evolution of each atomic hyperfine state on 3D space, which is defined by the pseudoangular momentum operators of each atomic hyperfine state $\hat{S}_{\sigma x} = \frac{1}{2}(\hat{a}_{l\sigma}^\dagger \hat{a}_{r\sigma} + \hat{a}_{r\sigma}^\dagger \hat{a}_{l\sigma})$, $\hat{S}_{\sigma y} = \frac{1}{2i}(\hat{a}_{l\sigma}^\dagger \hat{a}_{r\sigma} - \hat{a}_{r\sigma}^\dagger \hat{a}_{l\sigma})$, and $\hat{S}_{\sigma z} = \frac{1}{2}(\hat{a}_{l\sigma}^\dagger \hat{a}_{l\sigma} - \hat{a}_{r\sigma}^\dagger \hat{a}_{r\sigma})$. In the mean-field approximation, one has the average value of the pseudoangular momentum $\langle \hat{S}_{\sigma xyz} \rangle \equiv S_{\sigma xyz}$ with $S_{\sigma xyz}$ being c numbers.

We first pay close attention to the transition from non-MS to MS dynamics caused by Raman laser intensity. Figures 1(a) and 1(b) show the evolution of three-dimensional (3D) space constructed by the average value of the pseudoangular momentum operators $S_{\sigma x}$, $S_{\sigma y}$, and $S_{\sigma z}$. In the figure, we take $J = 0.3$, $g = 0.6$, and $g_{\uparrow\downarrow} = 0.0$ as an example. Hereafter, we establish that all bosons with equal spin-up and spin-down are prepared initially, and also have $S_{\uparrow z}(0) = 0.1$ and $S_{\downarrow z}(0) = 0.05$. For weak Raman laser intensity, $\Omega = 0.008$, the domain covered during the evolution of two atomic hyperfine states is separated in 3D phase space [Fig. 1(a)], i.e., the system displays non-MS dynamics. However, the system presents MS dynamics for strong Raman laser intensity. As seen in Fig. 1(b), $\Omega = 0.01$, the two clouds share the same phase space [Fig. 1(b)].

Figures 1(c) and 1(d) show the evolution of $S_{\sigma z}$ for each atomic hyperfine state. In the figure, the system parameters in Figs. 1(c) and 1(d) are in complete agreement with those in Figs. 1(a) and 1(b), respectively. We note that the dynamics of each atomic hyperfine state presents quasiperiodic oscillation. In the non-MS cases [Fig. 1(c)], the amplitudes of the oscillation are different for two atomic hyperfine states. In the MS cases, however, the amplitudes of the oscillation are the same for two atomic hyperfine states. The results demonstrate that the transition from non-MS to MS dynamics can be modulated by Raman laser intensity, even in the absence of interspin atomic interaction. In experiment, one

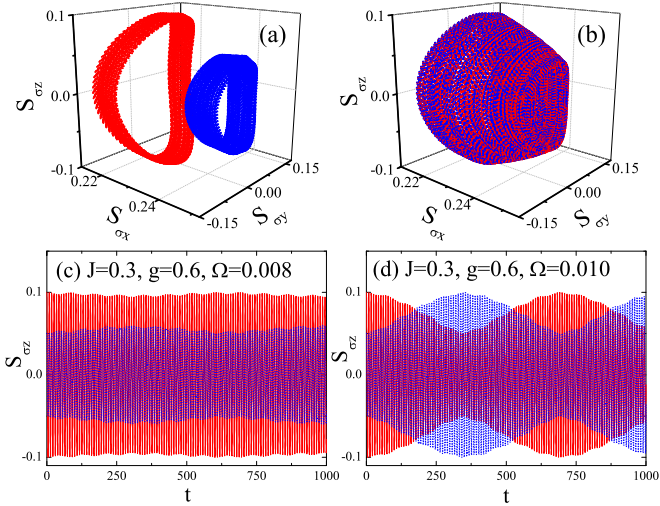


FIG. 1. (Color online) Measure synchronization with adjustable Raman laser intensity. Measure synchronization characterized by the domain covered during the evolution of each atomic hyperfine state on the 3D space defined by $S_{\sigma x}$, $S_{\sigma y}$, and $S_{\sigma z}$. Red circle (solid red line) and blue triangle (dotted blue line) correspond to two atomic hyperfine states spin-up $|\uparrow\rangle$ and spin-down $|\downarrow\rangle$, respectively. (a) and (b) The evolution of three-dimensional space. (c) and (d) The evolution of $S_{\sigma z}$. (a) and (c) $\Omega = 0.008$ for non-MS dynamics, (b) and (d) $\Omega = 0.010$ for MS dynamics. The other system parameters are $J = 0.3$, $g = 0.6$, and $g_{\uparrow\downarrow} = 0.0$.

can measure the transitions from non-MS to MS by observing the amplitudes of the quasiperiodic oscillation for two atomic hyperfine states.

The transition from non-MS to MS dynamics is related to the energy exchange between the two atomic hyperfine states spin-up $|\uparrow\rangle$ and spin-down $|\downarrow\rangle$ [16–18]. In non-MS dynamics, the energy exchange between the two atomic hyperfine states is finite. However, total energy is exchanged between the two atomic hyperfine states in MS dynamics. In the mean-field theory, we can obtain the energies for each atomic hyperfine state as $E_\sigma = \langle \hat{H}_\sigma \rangle$. In Fig. 2, we plot the energy functions for each atomic hyperfine state with different Raman laser intensities. For weak Raman laser intensity, the system exhibits non-MS dynamics [Fig. 2(a)], and the evolutions of energies E_\uparrow and E_\downarrow do not overlap at all. When the Raman laser intensity becomes larger than a critical value, E_\uparrow and E_\downarrow suddenly have the same range, and the system exhibits MS dynamics [Fig. 2(b)].

The transition from non-MS to MS dynamics can be clearly seen by looking at the time average of the energies of each atomic hyperfine state $\langle E_\uparrow \rangle$ and $\langle E_\downarrow \rangle$. The average energy of a single atomic hyperfine state is defined as

$$\langle E_\sigma \rangle = \frac{1}{T} \int_0^T E_\sigma dt. \quad (3)$$

In Fig. 3(a), we show the average energies $\langle E_\uparrow \rangle$ and $\langle E_\downarrow \rangle$ as a function of Raman laser intensity Ω . It is clear that there is a transition at $\Omega = \Omega^* = 0.0086$. For weak Raman laser intensity, $\Omega < \Omega^*$, there is a finite difference between $\langle E_\uparrow \rangle$ and $\langle E_\downarrow \rangle$, clearly indicating non-MS. When the Raman laser intensity is larger than the critical value, $\Omega > \Omega^*$, both

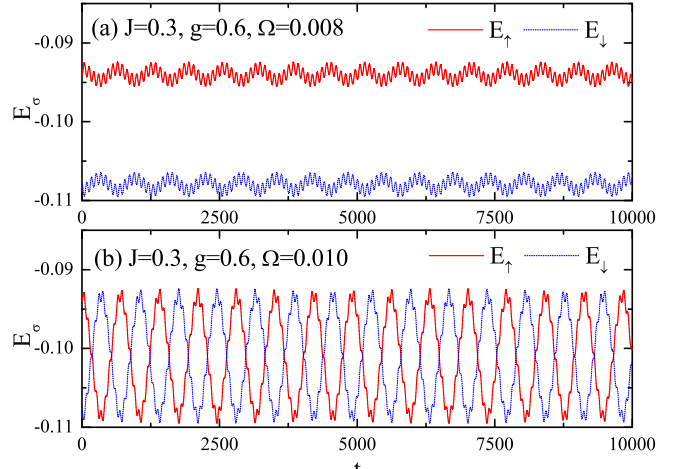


FIG. 2. (Color online) Evolution of energies for the two atomic hyperfine states spin-up $|\uparrow\rangle$ and spin-down $|\downarrow\rangle$. Transition from non-MS to MS dynamics is achieved by energy exchange between the two atomic hyperfine states. The total and finite energies are exchanged between the two atomic hyperfine states for the system displays of MS and non-MS dynamics, respectively. System parameters are the same as in Fig. 1.

atomic hyperfine states have identical average energies, clearly indicating MS.

The critical value for the transition from non-MS to MS dynamics is also dependent on the Josephson tunneling amplitude J . Figure 3(b) shows the phase diagram of non-MS and MS dynamics as functions of Raman laser intensity Ω and Josephson tunneling amplitude J . For a given Josephson tunneling amplitude J , there is always a critical Raman laser intensity Ω^* . The system displays non-MS or MS dynamics for Raman laser intensity weaker or stronger than the critical value, respectively. We also find that the critical Raman laser intensity Ω^* changes dramatically and slowly for weak and strong Josephson tunneling amplitude, respectively.

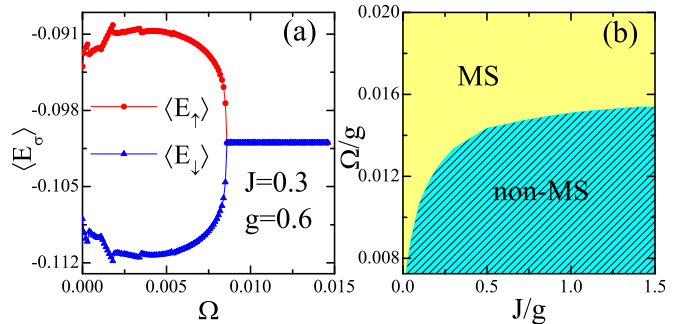


FIG. 3. (Color online) (a) Average energies of the two atomic hyperfine states vs Raman laser intensity. The two atomic hyperfine states have unequal and equal averaged energy for non-MS and MS. (b) Phase diagram as functions of Raman laser intensity and Josephson tunneling amplitude.

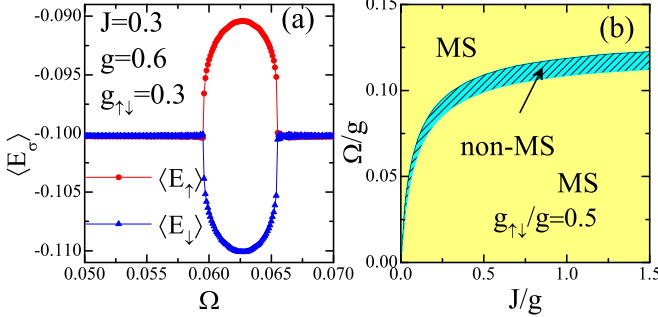


FIG. 4. (Color online) System parameters are the same as in Fig. 3 but with interspin atomic interaction $g_{\uparrow\downarrow}$. (a) Average energies of the two spin states vs Raman laser intensity. (b) Phase diagram as functions of Raman laser intensity and Josephson tunneling amplitude.

B. MS breaking dynamics

In this subsection, we investigate MS dynamics by considering both the Raman laser intensity Ω and the interspin atomic interaction $g_{\uparrow\downarrow}$, which couple the spin-up $|\uparrow\rangle$ and spin-down $|\downarrow\rangle$ system. The system displays MS breaking dynamics resulting from the competition between the intraspin atomic interaction $g_{\sigma\sigma}$ and the interspin atomic interaction $g_{\uparrow\downarrow}$.

In Fig. 4(a) we plot the average energies $\langle E_\sigma \rangle$ of each atomic hyperfine state as a function of Raman laser intensity Ω . To compare it with the case without interspin atomic interaction $g_{\uparrow\downarrow}$, we take system parameters the same as in Fig. 3 but with interspin atomic interaction $g_{\uparrow\downarrow} = 0.3$. Comparing Fig. 3(a) with Fig. 4(a), there are two critical Raman laser intensities Ω^* and Ω^{**} in Fig. 4(a). When the Raman laser intensity is weaker than the critical value Ω^* or stronger than the critical value Ω^{**} , the average energies of both atomic hyperfine states are equal, i.e., $\langle E_\uparrow \rangle = \langle E_\downarrow \rangle$, and the system exhibits MS dynamics. The system displays non-MS dynamics when adjusting the Raman laser intensity between the two critical values, i.e., $\Omega^* < \Omega < \Omega^{**}$.

By adjusting the Raman laser intensity, the system always exhibits MS dynamics apart from a window for non-MS dynamics. Figure 4(b) shows the phase diagram of MS breaking dynamics as a function of Raman laser intensity Ω and Josephson tunneling amplitude J . For very strong Raman laser intensity, no matter how strong the Josephson tunneling amplitude is, the system always exhibits MS dynamics. For relatively weak Raman laser intensity, the window of no-MS dynamics exists in the phase diagram. The width of the window changes dramatically and slowly for weak and strong Josephson tunneling amplitude, respectively.

To qualitatively explain the effect of system parameters on MS breaking dynamics, we show the phase diagram for MS and non-MS dynamics in Fig. 5. We find that the competition between the intraspin atomic interaction $g_{\sigma\sigma}$ and the interspin atomic interaction $g_{\uparrow\downarrow}$ plays a crucial role in MS breaking dynamics. For interspin atomic interaction stronger than intraspin atomic interaction, i.e., $g_{\uparrow\downarrow}/g_{\sigma\sigma} > 1$, the system always exhibits MS dynamics. For interspin atomic interaction weaker than intraspin atomic interaction, i.e., $g_{\uparrow\downarrow}/g_{\sigma\sigma} < 1$, the windows for MS breaking dynamics are presented in the phase

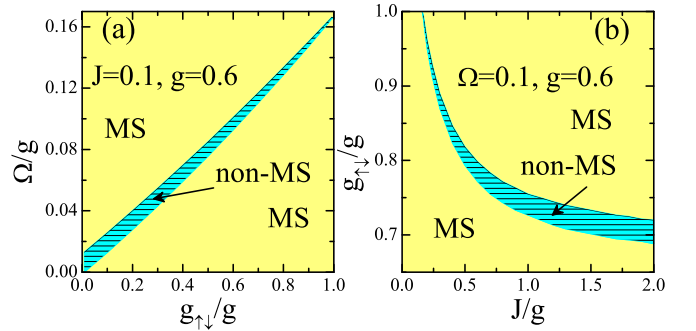


FIG. 5. (Color online) Phases for MS and non-MS (a) as functions of Raman laser intensity and interspin atomic interaction, and (b) as functions of Josephson tunneling amplitude and interspin atomic interaction.

diagram. We also find that the width of the window decreases with the increasing ratio of $g_{\uparrow\downarrow}/g_{\sigma\sigma}$.

IV. DISCUSSION AND CONCLUSION

Before concluding, we make some additional comments related to the double-well problem in the two-mode approximation. In this paper, we briefly discuss the weakly interacting case, which has been assumed to meet the requirement of a two-mode approximation. An accessible method to adjust the interaction parameters is to employ the tunable Feshbach resonance technique. To increase the atomic number within the two-mode regime, one can reduce the effective scattering length by Feshbach resonance. MS is defined as orbits of two coupled Hamiltonian systems cover the same region in the phase space with identical invariant measures. The transition from non-MS to MS in coupled Hamiltonian systems is characterized by coupling strength between the subsystems. The double-well problem in the two-mode approximation results in terms containing $\hat{a}_{r\sigma}^\dagger \hat{a}_{r\sigma} \hat{a}_{l\sigma}^\dagger \hat{a}_{l\sigma}$ [41]. In view of the terms containing $\hat{a}_{r\sigma}^\dagger \hat{a}_{r\sigma} \hat{a}_{l\sigma}^\dagger \hat{a}_{l\sigma}$, we have calculated that transition from non-MS to MS. It was found clearly that the measure synchronization is still in existence and the critical values for transition from non-MS to MS have just been shifted. Since the terms containing $\hat{a}_{r\sigma}^\dagger \hat{a}_{r\sigma} \hat{a}_{l\sigma}^\dagger \hat{a}_{l\sigma}$ cannot change the MS essentially, we have neglected the terms for simplicity in this paper.

In summary, we investigated the transition from non-MS to MS dynamics in an SOC bosonic Josephson junction. The transition from non-MS to MS dynamics is related to the energy exchange between the two atomic hyperfine states spin-up $|\uparrow\rangle$ and spin-down $|\downarrow\rangle$. The transitions can be characterized by the time average of the energies of each atomic hyperfine state. The time averages of the energies of two coupled subsystems have a finite difference and are identical for non-MS and MS dynamics, respectively. Without considering interspin atomic interaction, the transition from non-MS to MS dynamics of two coupled atomic hyperfine states is determined by Raman laser intensity. The dynamics of two coupled Hamiltonian systems is shown to exhibit a transition from non-MS to MS as the strength of Raman coupling increases. The critical Raman laser intensity of the

transition from non-MS to MS dynamics is dependent on the Josephson tunneling amplitude. The phase diagram of non-MS and MS dynamics as functions of Raman laser intensity and Josephson tunneling amplitude is given, which shows that the critical Raman laser intensity changes dramatically and slowly for weak and strong Josephson tunneling amplitude, respectively. When considering the interspin atomic interaction, the system displays MS breaking dynamics resulting from the competition between intraspin and interspin atomic interactions. The coupled subsystems always present MS dynamics when interspin atomic interactions dominate in the competition. For interspin atomic interaction weaker than intraspin atomic interactions, a windows for non-MS dynamics is presented. The phase diagrams for MS breaking dynamics are presented, which are helpful for controlling the measure synchronization of two atomic hyperfine states in the SOC bosonic Josephson junction. In experiment, one can measure

the transition from non-MS to MS by observing the amplitudes of the quasiperiodic oscillation for each atomic hyperfine state. Since spin-orbit-coupled Bose-Einstein condensates provide a powerful platform for studies on physical problems in various fields, the results presented in this paper may be helpful to investigate the collective coherent dynamical behavior in a spin-orbit-coupled bosonic Josephson junction.

ACKNOWLEDGMENTS

We thank H. Cao for his helpful suggestions. This work is supported by the National Fundamental Research Program of China (Contracts No. 2013CBA01502, No. 2011CB921503, and No. 2013CB834100) and the National Natural Science Foundation of China (Contracts No. 11374040, No. 11475027, No. 11274051, and No. 11125417).

-
- [1] C. Huygens, *Horologium Oscillatorium* (Muguet, Paris, 1673).
 - [2] U. E. Vincent, *New J. Phys.* **7**, 209 (2005).
 - [3] L. M. Pecora and T. L. Carroll, *Phys. Rev. Lett.* **64**, 821 (1990).
 - [4] M. G. Rosenblum, A. S. Pikovsky, and J. Kurths, *Phys. Rev. Lett.* **76**, 1804 (1996).
 - [5] M. G. Rosenblum, A. S. Pikovsky, and J. Kurths, *Phys. Rev. Lett.* **78**, 4193 (1997).
 - [6] S. Boccaletti and D. L. Valladares, *Phys. Rev. E* **62**, 7497 (2000).
 - [7] N. F. Rulkov, M. M. Sushchik, L. S. Tsimring, and H. D. I. Abarbanel, *Phys. Rev. E* **51**, 980 (1995).
 - [8] L. Kocarev and U. Parlitz, *Phys. Rev. Lett.* **76**, 1816 (1996).
 - [9] H. U. Voss, *Phys. Rev. Lett.* **87**, 014102 (2001).
 - [10] C. Masoller, *Phys. Rev. Lett.* **86**, 2782 (2001).
 - [11] A. Hampton and D. H. Zanette, *Phys. Rev. Lett.* **83**, 2179 (1999).
 - [12] J. R. Zhang, H. Jiang, Y. Yang, W. S. Duan, and J. M. Chen, *Phys. Scr.* **86**, 065602 (2012).
 - [13] U. E. Vincent, A. N. Njah, and O. Akinlade, *Mod. Phys. Lett. B* **19**, 737 (2005).
 - [14] X. Wang, Z. Ying, and G. Hu, *Phys. Lett. A* **298**, 383 (2002).
 - [15] X. Wang, M. Zhan, C. H. Lai, and H. Gang, *Phys. Rev. E* **67**, 066215 (2003).
 - [16] H. B. Qiu, J. Tian, and L. B. Fu, *Phys. Rev. A* **81**, 043613 (2010).
 - [17] J. Tian, H. B. Qiu, G. F. Wang, Y. Chen, and L. B. Fu, *Phys. Rev. E* **88**, 032906 (2013).
 - [18] H. Qiu, B. Juliá-Díaz, M. A. Garcia-March, and A. Polls, *Phys. Rev. A* **90**, 033603 (2014).
 - [19] Y. J. Lin, K. J. García, and I. B. Spielman, *Nature (London)* **471**, 83 (2011).
 - [20] J. Y. Zhang *et al.*, *Phys. Rev. Lett.* **109**, 115301 (2012).
 - [21] C. Qu, C. Hamner, M. Gong, C. Zhang, and P. Engels, *Phys. Rev. A* **88**, 021604(R) (2013).
 - [22] A. J. Olson, S. J. Wang, R. J. Niffenegger, C. H. Li, C. H. Greene, and Y. P. Chen, *Phys. Rev. A* **90**, 013616 (2014).
 - [23] C. Hamner, C. L. Qu, Y. P. Zhang, J. J. Chang, M. Gong, C. W. Zhang, and P. Engels, *Nat. Commun.* **5**, 4023 (2014).
 - [24] K. Jiménez-García, L. J. LeBlanc, R. A. Williams, M. C. Beeler, C. Qu, M. Gong, C. Zhang, and I. B. Spielman, *Phys. Rev. Lett.* **114**, 125301 (2015).
 - [25] P. Wang, Z. Q. Yu, Z. Fu, J. Miao, L. Huang, S. Chai, H. Zhai, and J. Zhang, *Phys. Rev. Lett.* **109**, 095301 (2012).
 - [26] L. W. Cheuk, A. T. Sommer, Z. Hadzibabic, T. Yefsah, W. S. Bakr, and M. W. Zwierlein, *Phys. Rev. Lett.* **109**, 095302 (2012).
 - [27] R. A. Williams, M. C. Beeler, L. J. LeBlanc, K. Jimenez-Garcia, and I. B. Spielman, *Phys. Rev. Lett.* **111**, 095301 (2013).
 - [28] D. W. Zhang, L. B. Fu, Z. D. Wang, and S. L. Zhu, *Phys. Rev. A* **85**, 043609 (2012).
 - [29] Z. F. Yu and J. K. Xue, *Phys. Rev. A* **90**, 033618 (2014).
 - [30] J. Struck, J. Simonet, and K. Sengstock, *Phys. Rev. A* **90**, 031601(R) (2014).
 - [31] M. A. Garcia-March, G. Mazzarella, L. Dell'Anna, B. Julia-Diaz, L. Salasnich, and A. Polls, *Phys. Rev. A* **89**, 063607 (2014).
 - [32] R. Citro and A. Naddeo, *Eur. Phys. J. Special Topics* **224**, 503 (2015).
 - [33] Y. P. Zhang, G. Chen, and C. W. Zhang, *Sci. Rep.* **3**, 1937 (2013).
 - [34] M. Gong, S. Tewari, and C. Zhang, *Phys. Rev. Lett.* **107**, 195303 (2011).
 - [35] H. Hu, L. Jiang, X.-J. Liu, and H. Pu, *Phys. Rev. Lett.* **107**, 195304 (2011).
 - [36] M. Aidelsburger, M. Atala, M. Lohse, J. T. Barreiro, B. Paredes, and I. Bloch, *Phys. Rev. Lett.* **111**, 185301 (2013).
 - [37] H. Miyake, G. A. Siviloglou, C. J. Kennedy, W. C. Burton, and W. Ketterle, *Phys. Rev. Lett.* **111**, 185302 (2013).
 - [38] M. C. Beeler *et al.*, *Nature (London)* **498**, 201 (2013).
 - [39] V. Galitski and I. B. Spielman, *Nature (London)* **494**, 49 (2013).
 - [40] J. D. Koralek, C. P. Weber, J. Orenstein, B. A. Bernevig, S. C. Zhang, S. Mack, and D. D. Awschalom, *Nature (London)* **458**, 610 (2009).
 - [41] R. Gati and M. K. Oberthaler, *J. Phys. B* **40**, R61 (2007).
 - [42] D. Peter, K. Pawłowski, T. Pfau, and K. Rzażewski, *J. Phys. B* **45**, 225302 (2012).
 - [43] T. Anker, M. Albiez, R. Gati, S. Hunsmann, B. Eiermann, A. Trombettoni, and M. K. Oberthaler, *Phys. Rev. Lett.* **94**, 020403 (2005).
 - [44] R. Gati, B. Hemmerling, J. Fölling, M. Albiez, and M. K. Oberthaler, *Phys. Rev. Lett.* **96**, 130404 (2006).
 - [45] E. Boukobza, Michael G. Moore, D. Cohen, and A. Vardi, *Phys. Rev. Lett.* **104**, 240402 (2010).

- [46] F. Dalfovo, S. Giorgini, L. P. Pitaevskii, and S. Stringari, *Rev. Mod. Phys.* **71**, 463 (1999).
- [47] I. Bloch, J. Dalibard, and W. Zwerger, *Rev. Mod. Phys.* **80**, 885 (2008).
- [48] J. Javanainen, *Phys. Rev. Lett.* **57**, 3164 (1986).
- [49] G. J. Milburn, J. Corney, E. M. Wright, and D. F. Walls, *Phys. Rev. A* **55**, 4318 (1997).
- [50] A. Smerzi, S. Fantoni, S. Giovanazzi, and S. R. Shenoy, *Phys. Rev. Lett.* **79**, 4950 (1997); S. Raghavan, A. Smerzi, S. Fantoni, and S. R. Shenoy, *Phys. Rev. A* **59**, 620 (1999).
- [51] S. Giovanazzi, A. Smerzi, and S. Fantoni, *Phys. Rev. Lett.* **84**, 4521 (2000).
- [52] S. Levy, E. Lahoud, I. Shomroni, and J. Steinhauer, *Nature (London)* **449**, 579 (2007).
- [53] M. Albiez, R. Gati, J. Fölling, S. Hunsmann, M. Cristiani, and M. K. Oberthaler, *Phys. Rev. Lett.* **95**, 010402 (2005).
- [54] L. J. LeBlanc, A. B. Bardon, J. McKeever, M. H. T. Extavour, D. Jervis, J. H. Thywissen, F. Piazza, and A. Smerzi, *Phys. Rev. Lett.* **106**, 025302 (2011).
- [55] T. Betz, S. Manz, R. Bücker, T. Berrada, C. Koller, G. Kazakov, I. E. Mazets, H. P. Stimming, A. Perrin, T. Schumm, and J. Schmiedmayer, *Phys. Rev. Lett.* **106**, 020407 (2011).
- [56] I. I. Satija, R. Balakrishnan, P. Naudus, J. Heward, M. Edwards, and C. W. Clark, *Phys. Rev. A* **79**, 033616 (2009).
- [57] L. Zhou, H. Pu, and W. P. Zhang, *Phys. Rev. A* **87**, 023625 (2013).
- [58] W. S. Cole, S. Z. Zhang, A. Paramekanti, and N. Trivedi, *Phys. Rev. Lett.* **109**, 085302 (2012).
- [59] D. Pesin and L. Balents, *Nat. Phys.* **6**, 376 (2010).